ELSEVIER

Physica D 80 (1995) 333–355

PHYSICA D

Propagative Sine–Gordon solitons in the spatially forced Kelvin–Helmholtz instability

Olivier Pouliquen, Patrick Huerre, Jean-Marc Chomaz

Laboratoire d'Hydrodynamique (LadHyX), Ecole Polytechnique, F-91128 Palaiseau Cedex, France

Received 4 June 1993; revised 27 July 1994; accepted 9 September 1994
Communicated by L. Kramer

Abstract

The spatio-temporal evolution of the vortex sheet separating two finite-depth layers of immiscible fluids is examined in the vicinity of threshold when spatially periodic forcing is imposed at the horizontal boundaries. As a result of the Galilean invariance of the problem, the interface deformation is shown to satisfy a coupled system of evolution equations involving not only the usual "short-wave" at the critical wavenumber but also a shallow-water "long-wave" associated with the mean elevation of the interface. The weakly nonlinear model is further studied in the Boussinesq approximation where it reduces to a forced Klein–Gordon equation. Thus, the secondary Benjamin–Feir instability of nonlinear Stokes wavetrains is analysed in the absence of forcing. When spatial forcing is reintroduced, the competition between the imposed external length scale and the natural length scale of the interface is shown analytically to give rise to one-dimensional propagating Sine–Gordon phase solitons. Numerical simulations of the Klein–Gordon evolution model fully confirm this prediction and also lead to the determination of the range of stability of phase solitons.

1. Introduction

In a wide class of *dissipative* systems, spatially-periodic structures arise as a result of a primary instability that develops above a critical value of a control parameter. Such fully nonlinear structures are themselves subjected to secondary instabilities which may take the form of phase modulations of the primary patterns, as documented both experimentally and theoretically [1–4]. In Rayleigh–Bénard convection for example, convective rolls can become unstable to longitudinal phase modulations in a certain range of roll wavelengths. This instability, associated with the name of Eckhaus [5], leads to the disappearance of a roll, an event which brings the periodic pattern back into a stable domain of parameter space [6,7]. A similar evolution is also observed in Taylor–Couette flow between concentric cylinders [8,9].

The same type of secondary instability takes place in *conservative* systems such as deep water-gravity waves, and it is then associated with the name of Benjamin and Feir [10]. In particular it has been shown that nonlinear plane wavetrains governed by the cubic nonlinear Schrödinger equation are also unstable to phase modulations. But in contrast to the case of dissipative systems, the subsequent nonlinear evolution does not result in an irreversible change to a new stationary stable pattern. Instead, one observes finite-amplitude modulations that arise from a periodic exchange of energy between a finite number of sideband modes of the primary wave [11]. This succession of modulation and demodulation cycles is commonly

SSDI 0167-2789(94)00197-9

known as the Fermi–Pasta–Ulam (FPU) recurrence phenomenon [12] and it is made possible by the absence of viscous dissipation. As demonstrated by Stuart and Di Prima [13], the Benjamin–Feir and Eckhaus instabilities correspond to two limiting cases of a wider class of secondary phase instabilities that arise within the context of the one-dimensional Ginzburg–Landau equation.

More fundamentally phase instabilities are intimately related to the continuous translational symmetry of the underlying basic system [2,14]. The spatially periodic pattern naturally breaks this continuous symmetry, but the phase invariance associated with arbitrary displacements of the pattern is responsible for the existence of a long wavelength neutral phase mode that can become unstable under certain conditions.

Continuous translational invariance may also be broken externally by forcing the system in a spatially periodic fashion so as to strongly affect the development of the phase instabilities. This situation is tantamount to the study of the competition between an externally imposed length scale and the natural wavelength of the system. Convection experiments in nematics [15,16] have indicated that spatially periodic forcing leads to a commensurate–incommensurate transition [17] signaled by the appearance of soliton-like phase envelopes. The phase dynamics analysis "à la Kuramoto" developed by Coullet and Repaux [20], Coullet [18] and Coullet and Huerre [19] near the threshold of instability provides a satisfactory description of this transition and it manages to capture the soliton-like phase behavior in the case of Rayleigh–Bénard convection.

The present theoretical investigation was initially motivated by recent experimental results on the spatially forced Kelvin–Helmholtz instability performed in our laboratory [21]. The experiment consists in creating a uniformly accelerating shear flow by tilting a long tube filled with two immiscible fluids of different densities [22]. External forcing is produced by periodically modulating the upper or lower boundary of the tube with small obstacles. As in the convection experiments of Lowe and Gollub [15,16], phase solitons are observed as a result of the competition between the natural wavelength of the interface and the imposed wavelength. Note, however, that the dynamics of the interface in the Kelvin–Helmholtz experiments are essentially *conservative* and that the *dissipative* model in [18,19] is not applicable.

The aim of the present study is therefore to present a phase dynamics analysis of the effects of spatial forcing on the inviscid evolution of Kelvin–Helmholtz instability waves, and thereby to demonstrate that wavelength competition leads to the formation of Sine–Gordon phase solitons. We restrict our attention to the case of a vortex sheet separating two uniform streams of finite depth, a periodic modulation being applied to the lower boundary.

The one-dimensional amplitude equations governing the evolution of the interface near instability onset are outlined in Section 2, detailed calculations being relegated to Appendix A. The analysis is the extension of Weissman's study [23] to the case of finite fluid layers with periodic forcing. The presence of solid boundaries at a finite distance leads to long wave–short wave interactions, the amplitude of nearly neutral interfacial waves being coupled to three additional large-scale fields: the mean elevation of the interface and mean corrections to the basic horizontal velocity in each layer. However, under the Boussinesq approximation, the long wavelength fields become decoupled from the short wave amplitude and they can be set equal to zero. The amplitude evolution model is then reduced to a nonlinear Klein–Gordon equation which has been derived in other conservative problems such as the buckling of elastic shells [24], baroclinic instability waves [25], or instabilities in slender accretion disks [26]. The sensitivity of nonlinear plane wave solutions to disturbances of the Benjamin–Feir–Eckhaus type is examined in Section 3. In the linear analysis, use is made of the general result obtained by Newton and Keller [27,28] for a generic form of differential equations. The corresponding finite-amplitude régime is then determined by resorting to direct numerical simulations of the Klein–Gordon equation. Finally, in Section 4 , it is demonstrated that the phase dynamics of nonlinear plane waves are governed by a Sine–Gordon equation admitting propagating soliton solutions when spatial forcing is applied. Final remarks

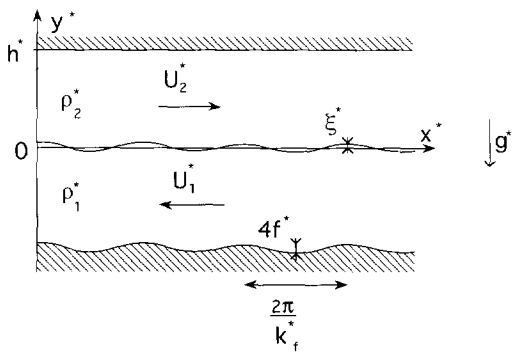

Fig. 1. Sketch of basic flow.

and comparison with experiments are included in Section 5.

2. Amplitude evolution equations

As first proposed by Lord Kelvin in 1871 [29], we consider the instability of the interface separating two streams of immiscible inviscid fluids in relative two-dimensional motion (Fig. 1). All dimensional and nondimensional quantities are indicated by starred and unstarred variables respectively. The velocity and density of the basic flow are uniform in each layer and denoted by U_1^*, ρ_1^* in the lower layer and U_2^*, ρ_2^* in the upper layer, with $\rho_1^* \geq \rho_2^*$. Surface tension between the two fluids is equal to γ^*. The upper solid boundary at $y^* = h^*$ is kept plane and horizontal while the lower boundary is modulated and of the form $y^* = -h^* + 2f^* \cos(k_f^* x^*)$, where f^* and k_f^* characterize the forcing amplitude and wavenumber respectively. In the sequel, the forcing amplitude f^* will be assumed small so that, at leading order, the basic flow is indeed unidirectional as depicted in Fig. 1.

This configuration provides a simplified model of the set-up used in the spatially-forced temporal mixing layer experiments reported in [21]. As in Weissman [23], dimensionless variables are defined with respect to the density scale

$$\rho^* = \rho_1^* + \rho_2^* ,$$

the capillary length scale

$$L^* = \sqrt{\frac{\gamma^*}{g^*(\rho_1^* - \rho_2^*)}} ,$$

and the velocity scale

$$V^* = \left(\frac{\sqrt{\gamma^* g^* (\rho_1^* - \rho_2^*)}}{\rho_1^* + \rho_2^*} \right)^{1/2} ,$$

where g^* denotes gravity. The flow is then governed by six dimensionless parameters: the density ratio $\rho_1 = \rho_1^*/\rho^*$, the dimensionless depth of the fluid layers $h = h^*/L^*$, the scaled velocities in each layer $U_i = U_i^*/V^*, i = 1,2$, the scaled forcing amplitude $f = f^*/L^*$ and wavenumber $k_f = k_f^* L^*$.

A straightforward linear stability analysis of the basic flow in the absence of forcing leads to the dispersion relation:

$$D(\sigma, k, U_1, U_2) \equiv -\left[\sigma + ik\left(\rho_1 U_1 + \rho_2 U_2\right)\right]^2 + \rho_1 \rho_2 k^2 (\Delta U)^2 - (k + k^3) \tanh(kh) = 0 , \quad (1)$$

where σ is the complex temporal growth rate of interface deformations of the form $\xi \sim \exp(ikx + \sigma t)$, $k = k^* L^*$ being the dimensionless wavenumber and $\Delta U \equiv U_2 - U_1 = \left(U_2^* - U_1^*\right)/V^*$ the dimensionless velocity difference [30]. The neutral curve in the $k - \Delta U$ plane sketched on Fig. 2 is defined by the condition $D_\sigma = 0$, where D_σ denotes the derivative of the dispersion relation with respect to σ. Its shape results from the combination of two stabilizing effects: the density difference at large wavelengths (small k) and surface tension at short wavelengths (large k). The onset of the Kelvin–Helmholtz instability is seen to take place at a well-defined critical wavenumber k_c above a value ΔU_c of the scaled velocity difference. This critical point is defined by the relations

$$D_\sigma = D_k = 0 .$$

As shown in Appendix A, these relations yield a nonzero value of the critical wavenumber k_c as long as the scaled depth h is larger than $\sqrt{3}$. Under this assumption, which will be made throughout, σ takes the specific value

$$\sigma_c = -i\left(\rho_1 U_{1_c} + \rho_2 U_{2_c}\right) k_c ,$$

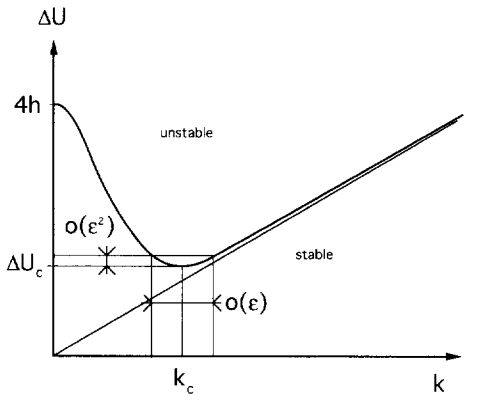

Fig. 2. Neutral curve of the Kelvin–Helmholtz instability in the nondimensional wavenumber-velocity difference plane.

which corresponds to traveling waves of phase speed equal to $\rho_1 U_{1_c} + \rho_2 U_{2_c}$.

The objective of this section is to carry out a weakly nonlinear analysis in the vicinity of the neutral point k_c, ΔU_c when instability waves are forced by the stationary modulated lower boundary. Resonance between the neutral wave and the stationary spatial perturbation can only occur if both disturbances have equal propagation velocities, i.e. if the phase velocity at critical satisfies the condition

$$\rho_1 U_{1_c} + \rho_2 U_{2_c} = 0 . \tag{2}$$

Under this assumption, which will hold in the entire study, the dispersion relation depends only on the velocity difference ΔU and no longer on the individual velocities U_i so that one can express (1) in the form $D(\sigma, k, \Delta U) = 0$. A complete derivation of the system of amplitude equations is given in Appendix A.

Following Weissman [23], we introduce an $\mathcal{O}(1)$ supercriticality parameter Δ such that

$$\Delta U = \Delta U_c + \Delta\, \varepsilon^2 ,$$

where $\varepsilon \ll 1$ denotes the order of magnitude of the interface deformation $\xi(x,t)$. The interface elevation is then expanded in the form

$$\xi = \varepsilon \xi^{(1)} + \varepsilon^2 \xi^{(2)} + \varepsilon^3 \xi^{(3)} + \cdots ,$$

with

$$\xi^{(1)} = A(X,T)\, e^{i(k_c x)} + \text{c.c.}$$

The complex amplitude $A(X,T)$ is an unknown function of the slow space and time variables X and T defined by

$$(X,T) = \varepsilon(x,t) ,$$

this particular choice being motivated by the fact that close to ΔU_c, the linear growth rate is proportional to $(\Delta U - \Delta U_c)^{1/2}$ and the width of the unstable band of wavenumbers is also of order $(\Delta U - \Delta U_c)^{1/2}$. Note that the amplitude evolution time scale is $\mathcal{O}\left(\varepsilon^{-1}\right)$ and not $\mathcal{O}\left(\varepsilon^{-2}\right)$ as in dissipative systems.

The spatially periodic modulation imposed to the lower boundary is assumed to be nearly resonant so that

$$k_f = k_c + q\, \varepsilon ,$$

where the $\mathcal{O}(1)$ parameter q is a measure of the detuning between k_f and k_c. Finally the strength of the small forcing amplitude f is chosen in such a way as to appear at the same order as the anticipated nonlinear term $|A|^2 A$ in the amplitude equation. The shape of the lower boundary is therefore taken to be

$$y = -h + \varepsilon^3 F_0 e^{i(k_c + q\varepsilon)x} + \text{c.c.} ,$$

with F_0 and q being $\mathcal{O}(1)$.

As outlined in Appendix A, in order to obtain a closed system of amplitude evolution equations one needs to solve the Laplace equation and associated boundary and interface conditions to order ε^3 included. In contrast to the infinite depth case studied by Weissman [23], the evolution of the carrier wave at k_c is found to be strongly coupled to two large-scale velocity fields $\mathcal{U}_1(X,T)$ and $\mathcal{U}_2(X,T)$ in each of the fluid layers and to the associated large-scale elevation of the interface $\mathcal{H}(X,T)$. These long wavelength fields are $\mathcal{O}(\varepsilon^2)$ and compatibility conditions at $\mathcal{O}(\varepsilon^2)$ and $\mathcal{O}(\varepsilon^3)$ lead to the following coupled system:

$$\left(\frac{\partial}{\partial T} + U_{2_c}\frac{\partial}{\partial X}\right)\mathcal{H} - h\frac{\partial \mathcal{U}_2}{\partial X} = 0 , \tag{3a}$$

$$\left(\frac{\partial}{\partial T} + U_{1_c}\frac{\partial}{\partial X}\right)\mathcal{H} + h\frac{\partial \mathcal{U}_1}{\partial X} = 0 , \tag{3b}$$

$$\frac{\partial \mathcal{H}}{\partial X} - \left(\frac{\partial}{\partial T} + U_{2_c}\frac{\partial}{\partial X}\right)\rho_2 \mathcal{U}_2$$

$$+\left(\frac{\partial}{\partial T}+U_{1_c}\frac{\partial}{\partial X}\right)\rho_1\mathcal{U}_1 = S\frac{\partial|A|^2}{\partial X}, \tag{3c}$$

$$-\frac{1}{2}D_{\sigma\sigma}\frac{\partial^2 A}{\partial T^2}+\frac{1}{2}D_{kk}\frac{\partial^2 A}{\partial X^2} = \Delta D_{\Delta U}A + N|A|^2A + Fe^{iqX} + 2k_c^2\left(\rho_1 U_{1_c}\mathcal{U}_1 + \rho_2 U_{2_c}\mathcal{U}_2\right)A - R\mathcal{H}A. \tag{3d}$$

The form of the linear operator appearing in (3d) reflects the nature of the dispersion relation (1) in the vicinity of critical. In fact, the constant coefficients $D_{\sigma\sigma}$, $D_{\sigma k}$ D_{kk} and $D_{\Delta U}$ multiplying the various linear terms of (3d) refer to the corresponding derivatives of the dispersion relation (1) evaluated at $k_c, \Delta U_c$. Expressions for the coefficients N, R and S of the various non-linear terms appearing in (3c) and (3d) and for the scaled forcing amplitude F are given in Appendix A (Eqs. (A.9), (A.16)–(A.19)). Note that if $\rho_1 U_{1_c} + \rho_2 U_{2_c} \neq 0$, the phase velocity at critical would not be zero and the forcing term on the right-hand side of (3d) would be absent, since there is no strong interaction with external forcing, furthermore an extra term $D_{\sigma k}\partial^2 A/\partial X\partial T$ would appear on the left-hand side of (3d) to account for finite group velocities.

The evolution of the large scale fields $\mathcal{U}_1, \mathcal{U}_2$ and $\mathcal{H}$ is primarily governed by Eqs. (3a)–(3c) which can be recognized as a system of shallow-water wave equations linearised around the basic flow U_{1_c}, U_{2_c}. More specifically, (3a) and (3b) express mass conservation of the mean flow in each fluid layer whereas (3c) is a statement of conservation of momentum along the x-direction. According to the right-hand side of (3c), the large scale fields are induced by spatial inhomogeneities in the amplitude $|A(X,T)|$ of the Kelvin–Helmholtz wavetrain.

The evolution of the amplitude $A(X,T)$ associated with the carrier wavenumber k_c is primarily governed by the forced Klein–Gordon Eq. (3d). The effect of the prescribed spatially periodic modulation is contained in the driving term Fe^{iqX}. Finite values of the mean fields $\mathcal{U}_1, \mathcal{U}_2$ and $\mathcal{H}$ are seen to shift the effective value of the threshold of instability, as reflected by the coupling terms involving $\mathcal{H}A, \mathcal{U}_1 A$ and $\mathcal{U}_2 A$ on the right-hand side of (3d).

The simultaneous occurrence of a nearly neutral mode $A(X,T)$ of finite wavenumber k_c, and of nearly neutral modes $\mathcal{H}(X,T), \mathcal{U}_1(X,T), \mathcal{U}_2(X,T)$ at $k \sim 0$ is intimately related with the symmetry properties of the underlying system. More specifically, in the absence of forcing, the problem under consideration is not only invariant under arbitrary space translations $x \to x + \text{const.}$, but also under Galilean transformations $x \to x - Ut$. Following the same arguments as in Coullet and Fauve [14], one may therefore expect a constant velocity field in each layer to also be a neutral mode of the system. In the presence of a density interface, long wavelength variations $\mathcal{U}_1$, $\mathcal{U}_2$ of this constant velocity field are likely to produce, by mass conservation, slight modulations $\mathcal{H}$ of the surface elevation. Thus the dynamics near threshold involve coupling between a neutral mode of complex amplitude $A(X,T)$ at wavenumber k_c and two long wavelength neutral modes $\mathcal{U}_1(X,T)$ and $\mathcal{U}_2(X,T)$ at $k \sim 0$. The relationship between the nature of long wave-short wave interactions at a fluid interface and the invariance properties of the underlying system was initially identified by Chomaz et al. [31]. An evolution model closely related to system (3) has recently been obtained by Pavithran and Redekopp [32,33] in the context of Rayleigh–Bénard convection in a horizontal fluid layer with a free interface. The finite wavenumber mode is then associated with the convective rolls near threshold whereas the large-scale field corresponds to "shallow-water" waves at the interface. In contrast with the case under consideration here, the dynamics are strongly dissipative and the time-reversible Klein–Gordon operator in (3d) is replaced by a first-order in time Ginzburg–Landau equation. For other examples of long wave-short wave interactions at an interface, the reader is referred to Davey and Stewartson [34], Djordjevic and Redekopp [35], Ma and Redekopp [36] and Renardy and Renardy [37] among others.

It should also be emphasized that system (3) is fully compatible with the result obtained by Weissman [23] in the case of infinitely deep fluid layers. If one lets h become infinite in (3) the coefficient S multiplying the coupling term $\partial|A|^2/\partial X$ in (3c) becomes zero as readily seen from Eq. (A.9) in Appendix A. Thus, the large-scale field is uncoupled from the evolution of A and one may assume, without loss of generality, that $\mathcal{U}_1(X,T) = \mathcal{U}_2(X,T) = \mathcal{H}(X,T) = 0$. Finally, the

forcing coefficient F defined in (A.17) also becomes zero in the limit $h \to \infty$ and system (3) then reduces to the nonlinear Klein–Gordon equation analyzed by Weissman [23].

It is not the purpose of the present investigation to pursue in detail the study of the solutions of (3). Rather, we seek to isolate a subsystem of (3) which is valid under well-defined conditions and which is capable of describing, to leading-order, the competition between the imposed spatially periodic modulations and the "natural" instability of the interface. As in our previous work [38], we shall make the Boussinesq approximation. In the present situation, this assumption amounts to neglecting density variations except when they appear multiplying the gravity term. With the choice of nondimensional parameters adopted here, the Boussinesq approximation is equivalent to setting $\rho_1 = \rho_2 = 1/2$. In such a case, the resonance condition (2) reduces to $U_{1_c} = -U_{2_c}$ and the coupling term S on the right-hand side of (3c) vanishes, as seen from Eq. (A.9) in Appendix A. As before, one may set, without loss of generality $\mathcal{H} = \mathcal{U}_1 = \mathcal{U}_2 = 0$, but this time the forcing term remains finite. It can therefore be concluded that, *in the Boussinesq approximation*, the nonlinear evolution of wavepackets, in the presence of spatially periodic external modulations, is governed by the forced Klein–Gordon equation

$$-\frac{1}{2}D_{\sigma\sigma}\frac{\partial^2 A}{\partial T^2} + \frac{1}{2}D_{kk}\frac{\partial^2 A}{\partial X^2} = \Delta D_{\Delta U} A + N|A|^2 A + Fe^{iqX}, \tag{4}$$

where it is understood that all coefficients are evaluated at $\rho_1 = \rho_2 = 1/2$ (cf. Eqs. (A.20)–(A.21)). In the rest of the paper we shall restrict our attention to the study of (4). As stated in the introduction, the Klein–Gordon equation arises in a wide variety of situations: buckling of elastic shells [24], baroclinic instability [25], instability of accretion disks [26], among other applications. In all the above examples, dissipation is neglected and the reversible nature of the dynamics is expressed by the invariance under time reflections $t \to -t$, thereby accounting for the presence of the second-order time derivative $\partial^2 A/\partial T$ in (4). Note that a more general form of (4) including a dissipative first order time derivative term has been considered by Elphik [39] near a codimension-two bifurcation. Symmetry arguments are also helpful in justifying the form taken by the forcing term [18]. When external periodic modulations of wavenumber k_f are introduced, the continuous translational invariance $x \to x+\text{const.}$ is broken and replaced by the discrete translational symmetry $x \to x+2\pi n/k_f$, where n is an integer. For the complex amplitude $A(X,T)$, the latter is equivalent to the rotational symmetry $A \to Ae^{-2\pi i n q/k_c}$. The forcing term in (4) respects this symmetry property and it is identical to the corresponding term in forced thermal convection [19]. The nonlinear coefficient N depends on the properties of each basic stream. Under the conditions $\rho_1 = \rho_2 = 1/2$ and $U_{1_c} = -U_{2_c}$, one finds $N < 0$ as shown in Appendix A and this assumption will be made in the remainder of the study. For simplicity, the following change of variables is introduced:

$$X \to \frac{1}{\sqrt{-\frac{1}{2}D_{kk}}}X, \quad A \to \sqrt{-N}A,$$

$$q \to \sqrt{-\tfrac{1}{2}D_{kk}}\,q, \quad F \to \frac{1}{\sqrt{-N}}F,$$

with $\mu = \Delta D_{\Delta U}$. In terms of these scaled quantities, evolution Eq. (4) reads

$$\frac{\partial^2 A}{\partial T^2} - \frac{\partial^2 A}{\partial X^2} = \mu A - |A|^2 A + Fe^{iqX}, \tag{5}$$

where μ is the new supercriticality parameter and F and q denote the amplitude of the excitation and the wavenumber misfit respectively.

In order to explore the effect of forcing on the development of the instability and to illustrate some of the theoretical results to be presented in the following sections, the Klein–Gordon equation (5) is solved numerically in the case of periodic boundary conditions $A(X+L,T) = A(X,T)$ on an interval of length L. The spatial derivative is approximated by centered finite-differences, and the temporal evolution is incremented through a second-order predictor-corrector scheme of time step δt. A mesh of 80 equally spaced points is selected on the periodic interval, which corresponds to a spatial step $\delta x = L/80$. The accuracy of the numerical scheme and the amount of numerical dissipation

can be assessed by monitoring the temporal variations of the total energy

$$E=\int\left[\frac{1}{2}\left|\frac{\partial A}{\partial T}\right|^2+\frac{1}{2}\left|\frac{\partial A}{\partial X}\right|^2-\frac{\mu}{2}|A|^2+\tfrac{1}{2}|A|^4 -F\,\mathrm{Re}\left(Ae^{-iqX}\right)\right]dX,$$

over the interval L. The conservative Klein–Gordon Eq. (5) implies

$$\frac{dE}{dT}=0,$$

so that $E(t)$ should be conserved. In all the simulations to be presented in the following sections, numerical dissipation defined as $\Delta E/E(0) = [E(t) - E(0)]/E(0)$ does not exceed 3% over the entire duration of a run. The results are usually displayed on spatio-temporal $X-T$ diagrams such as in Fig. 4b. The total normalized interface deformation is then reconstructed by reintroducing a carrier wave of wavenumber k_c. More specifically, level contours of the interface elevation $2\mathrm{Re}\left(A(X,T)e^{ik_cX}\right)$ are represented on a gray scale in the $X-T$ plane, by arbitrarily setting $X = x$ and $\varepsilon = 1$.

3. Benjamin–Feir-Eckhaus instability of Stokes wavetrains

In this section the sideband instability of finite-amplitude wavetrain solutions of the Klein–Gordon equation (5) is examined in the absence of spatial forcing. The analysis is based on Benjamin and Feir's pioneering study of sideband instability in deep water gravity waves governed by the cubic nonlinear Schrödinger equation [10]. A similar formalism has been applied by Eckhaus [5] for dissipative systems such as convection rolls governed by the Newell–Whitehead equation [40]. We chose to follow here the methodology outlined by Newton and Keller [27,28] for a generalized Klein–Gordon equation with arbitrary potential.

Finite-amplitude Stokes solutions of (5) with $F = 0$ are sought in the form

$$A(X,T) = Qe^{i(qX-\omega T)}, \tag{6}$$

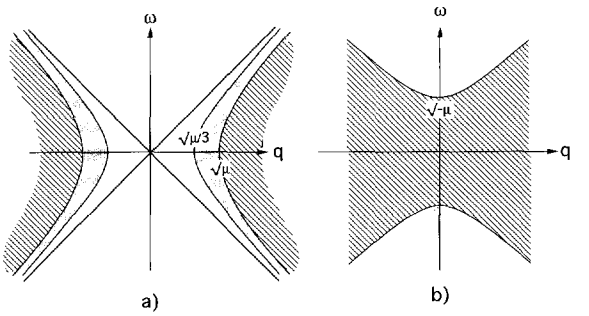

Fig. 3. Stability diagram of plane-wave solutions of the Klein–Gordon equation in the wavenumber q- frequency ω plane. Clear regions: stable plane waves; shaded regions: unstable plane waves; hatched regions: no plane waves (a) $\mu > 0$; (b) $\mu < 0$.

where Q is a real amplitude, ω is the frequency and q the wavenumber. By substituting (6) into (5), the domain of existence of nonlinear plane waves is found to be bounded by the hyperbola $\omega^2 - q^2 = -\mu$ in the $q-\omega$ plane. As shown on Figs. 3a and b for $\mu > 0$ and $\mu < 0$ respectively, no plane wave solutions can be obtained within the hatched areas.

Outside these regions, plane waves exist and their stability is examined by introducing sideband perturbations $\varphi(X,T)$ of wavenumber l and growth rate σ. The dispersion relation takes the form:

$$\sigma^4+\left[2(l^2+Q^2)+4\omega^2\right]\sigma^2+8i\omega ql\sigma+l^4 +l^2(2Q^2-4q^2)=0. \tag{7}$$

The nonlinear Stokes wavetrain of amplitude Q, wavenumber q and frequency ω will be unstable if there exists a sideband wavenumber l with a complex growth rate σ of positive real part. Eq. (7) is solved numerically with respect to σ at each point of the $q-\omega$ plane, for all values of the perturbation wavenumber l. The results are summarized in Figs. 3a,b: nonlinear plane waves are determined to be unstable within the dotted areas. It can be concluded that, below critical ($\mu < 0$), all existing plane waves are sideband stable (Fig. 3b). Above critical ($\mu > 0$), there are bands of unstable plane waves as indicated by the dotted zones in Fig. 3a. Eq. (7) may be solved analytically in certain cases. Thus, one finds that spatially uniform wavetrains $Qe^{-i\omega T}$ are always sideband stable. By contrast steady patterns Qe^{iqX} which may exist above critical ($\mu > 0$), are seen to be sideband

stable only in the range of wavenumbers

$$|q| < \sqrt{\tfrac{1}{3}\mu} \tag{8}$$

as indicated on Fig. 3a. When $|q| > \sqrt{\frac{1}{3}\mu}$, sideband wavenumbers l such that

$$|l| < \sqrt{6q^2 - 2\mu} \tag{9}$$

grow exponentially. It is interesting to note that the stability condition (8) is formally identical to the Eckhaus stability criterion applicable to steady convection rolls near threshold [40]. Note also that this sideband instability sets in at long wavelengths i.e. $l \ll 1$, when q is close to $\sqrt{\frac{1}{3}\mu}$ as in the classical Eckhaus case.

The finite-amplitude evolution of the secondary Benjamin–Feir instability may be investigated by introducing as initial conditions in the numerical simulations of Eq. (5) a stationary Stokes wavetrain Qe^{iqX} that is slightly perturbed. More specifically, the initial state is selected to be

$$A(X,0) = e^{iqX}\left[\sqrt{\mu - q^2} + \epsilon\varphi(X,0)\right],$$

$$\frac{\partial A}{\partial T}(X,0) = \epsilon\frac{\partial \varphi}{\partial T}(X,0)\, e^{iqX},$$

where

$$\varphi(X,T) = e^{\bar{\sigma}t - ilX} + \frac{(\sigma^2 - 2kl + l^2 + \mu - q^2)}{\mu - q^2}\, e^{\sigma t + ilX}$$

is the linearised eigenfunction of sideband wavenumber l and complex growth rate σ given by dispersion relation (7). The perturbation level is chosen to be $\varepsilon = 10^{-2}$. When the wavenumber q is within the stable range $|q| < \sqrt{\frac{1}{3}\mu}$, $\mu > 0$, perturbations remain negligibly small for all values of l, and a steady sinusoidal pattern Qe^{iqX} is observed. When the wavenumber q is in the unstable range $|q| > \sqrt{\frac{1}{3}\mu}$, sideband modes of wavenumber $q + l$ and $q - l$ grow in time as shown by the thin and bold curves in Fig. 4a. In this particular example, $q = l = 2\pi/L$ and $L = 16$, $\mu = 0.3$, so that $\pm l$ are the only discrete unstable sideband wavenumbers satisfying inequality (9). All other harmonics are stable. As seen from Fig. 4a, both sidebands $q + l$ and $q - l$ initially increase exponentially according to linear theory. However, the $q - l$ mode rapidly dominates and undergoes nearly time-periodic oscillations. The corresponding spatio-temporal evolution of the interface elevation $\xi = 2\mathrm{Re}\left(A(X,T)e^{ik_cX}\right)$ is represented on Fig. 4b with the value $k_c = 12\pi/L$ of the carrier wavenumber. In the transient regime, a spatio-temporal dislocation is seen to occur, which leads to the disappearance of a single wave trough and to an abrupt change of the mean wavenumber from $k_c + q$ to $k_c + q - l$. Beyond this initial phase, the energy content of all wavenumbers remains constant with the exception of $k_c + q$ and $k_c + q - l$ which experience a nearly periodic exchange of energy. In physical space (Fig. 4b), this energy transfer takes the form of periodic contractions and dilatations of the spatial pattern. As discussed in the introduction, similar finite-amplitude periodic modulations have been observed in other conservative systems and they are usually referred to by the name "FPU recurrence phenomenon" after Fermi, Pasta and Ulam [12]. For instance, the long-time nonlinear evolution of deep-water gravity wavetrains has been shown to exhibit FPU recurrence within the context of the cubic nonlinear Schrödinger equation [41]. Such an evolution equation is, incidentally, a pertinent finite-amplitude evolution model in the stable domain of the $k - \Delta U$ plane on Fig. 2, as demonstrated by Weissman [23]. The present results indicate that FPU dynamics also prevail in the vicinity of the threshold of instability.

4. Phase dynamics analysis of the Klein–Gordon equation

The secondary Benjamin–Feir instability which has just been investigated both analytically and numerically falls within the general class of phase instabilities. As emphasized by several authors [2,3,14,18], particularly in the case of dissipative systems, such instabilities are closely related to the translational symmetry $x \to x + \text{const.}$ of the governing equation. As a result of this invariance, the complex amplitude is defined up to an arbitrary phase which can be interpreted as a neutral mode of the system. Slow spatio-temporal

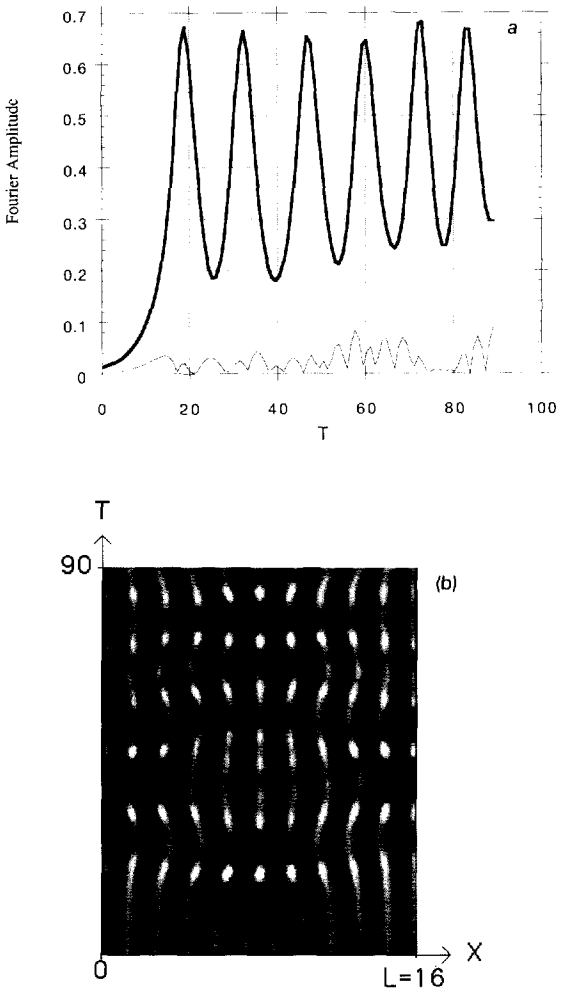

Fig. 4. Fermi-Pasta-Ulam recurrence in the Klein–Gordon equation. See Section 2 for the description of initial conditions. $\mu = 0.3$, $\delta x = 0.2$, $\delta t = 0.03$, $q = l = 2\pi/L$, $L = 16$. (a) Nonlinear time evolution of the amplitudes of the Benjamin–Feir unstable modes of respective wavenumber $q - l$ (bold line) and $q + l$ (thin line); (b) Spatio-temporal $X-T$ diagram of the elevation of the interface $\xi = 2\mathrm{Re}\left[A(X,T)e^{ik_c X}\right]$ of carrier wavenumber $k_c = 12\pi/L$. Darker (lighter) regions indicate the crests (troughs).

modulations of the neutral mode, i.e. phase dynamics, are likely to be amenable to analytical treatment via the method of multiple scales. The objective of the present section is to present such an analysis for the specific case of the Klein–Gordon equation, both unforced and forced. Our primary interest is in the phase dynamics of stationary plane waves ($\omega = 0$) which have the same wavenumber q as the spatial forcing.

The complex amplitude is written in the form

$$A(X,T) = \left[Q + \rho(X,T)\right] e^{i(qX+\theta(X,T))}, \tag{10}$$

where $\rho(X,T)$ and $\theta(X,T)$ denote amplitude and phase perturbations of the steady pattern Qe^{iqX} of wavenumber q and amplitude $Q = \sqrt{\mu - q^2}$. Upon substituting (10) into the Klein–Gordon equation with forcing (5), the following system of coupled equations is obtained for the dynamics of the perturbations $\rho(X,T)$ and $\theta(X,T)$:

$$\frac{\partial^2\rho}{\partial T^2} - (Q+\rho)\left(\frac{\partial\theta}{\partial T}\right)^2 = \mu(Q+\rho) + \frac{\partial^2\rho}{\partial X^2} - (Q+\rho)\left(\frac{\partial\theta}{\partial X} + q\right)^2 - (Q+\rho)^3 + F\cos(\theta), \tag{11a}$$

$$(Q+\rho)\frac{\partial^2\theta}{\partial T^2} + 2\frac{\partial\theta}{\partial T}\frac{\partial\rho}{\partial T} = (Q+\rho)\frac{\partial^2\theta}{\partial X^2} + 2\frac{\partial\rho}{\partial X}\left(\frac{\partial\theta}{\partial X} + q\right) - F\sin(\theta). \tag{11b}$$

The cases $F = 0$ and $F \neq 0$ are successively examined in Sections 4.1 and 4.2.

4.1. Free evolution

From the results of Section 2, stationary patterns are subject to the Benjamin–Feir instability when their wavenumber q satisfies $|q| > \sqrt{\frac{1}{3}\mu}$. A weakly-nonlinear phase dynamics analysis may be carried out in the vicinity of threshold $q_c = \sqrt{\frac{1}{3}\mu}$. Let $\delta \equiv q^2 - \frac{1}{3}\mu \ll 1$ be the small supercriticality parameter and $\varepsilon \ll 1$ the order of magnitude of the phase perturbations [1]. By exploiting the results of the linear analysis and the principle of the distinguished limit, one is led to adopt the following scaling relationships for δ, the slow time scale τ, the slow space scale η and the expansion of θ and ρ :

$$\delta = \varepsilon^2\Delta, \tag{12a}$$

$$\tau = \varepsilon^2 T, \tag{12b}$$

$$\eta = \varepsilon, \tag{12c}$$

[1] The parameter $\varepsilon \ll 1$ introduced here should not be confused whith the small parameter ε that defines the order of magnitude of the *primary* perturbations in Section 2.

$$\theta = \varepsilon\Theta_1 + \varepsilon^2\Theta_2 + \cdots , \tag{12d}$$

$$\rho = \varepsilon^2\rho_2 + \varepsilon^3\rho_3 + \cdots , \tag{12e}$$

where Δ, Θ_1, Θ_2, ρ_1, ρ_2, $\cdots$ are all $\mathcal{O}(1)$ quantities.

One is led, without difficulty from Eqs. (11a,b) to the following Boussinesq equation for the dynamics of the phase $\Theta_1(\eta,\tau)$:

$$\frac{\partial^2\Theta_1}{\partial\tau^2} = \frac{-3\Delta}{2q^2}\frac{\partial^2\Theta_1}{\partial\eta^2} - \frac{1}{4q^2}\frac{\partial^4\Theta_1}{\partial\eta^4} - \frac{3}{q}\frac{\partial\Theta_1}{\partial\eta}\frac{\partial^2\Theta_1}{\partial\eta^2} . \tag{12}$$

The properties of this evolution equation will not be examined here.

4.2. Forced evolution

As shown in [18,19], spatially-periodic forcing of *dissipative* systems supporting steady-periodic patterns may lead to the formation of stationary or propagating phase solitons. Such objects are produced in the vicinity of commensurate- incommensurate transitions [17] resulting from the competition between an externally imposed length scale and the intrinsic length scale of the system. The stationary soliton model [18] has been shown in particular to adequately describe forced convection experiments in nematics [15,16]: phase solitons then correspond to a localized compression of the rolls.

The objective here is to show that phase solitons are also generated when a *conservative* system, namely the Klein–Gordon equation, is spatially-forced. Let $F \ll 1$ denote the weak forcing amplitude. We consider the case of a Benjamin–Feir stable stationary pattern Qe^{iqX} of wavenumber such that $|q| < \sqrt{\frac{1}{3}\mu}$. In contrast with the unforced case, there is no restriction imposed on the level of supercriticality. In order to "catch" the effect of forcing at the same order as the leading linear terms, the following scaling relations are introduced:

$$\tau = \varepsilon T , \tag{13a}$$

$$\eta = \varepsilon X , \tag{13b}$$

$$F = \varepsilon^2\mathcal{F} , \tag{13c}$$

$$\theta = \Theta_0 + \varepsilon\Theta_1 + \cdots , \tag{13d}$$

$$\rho = \varepsilon\rho_1 + \varepsilon^2\rho_2 + \cdots , \tag{13e}$$

where $\mathcal{F}$, Θ_0, Θ_1, ρ_1, ρ_2 are all of order unity. Note that phase perturbations are now $\mathcal{O}(1)$. System (11) leads to the following evolution equation for the phase:

$$\frac{\partial^2\Theta_0}{\partial\tau^2} = c^2\frac{\partial^2\Theta_0}{\partial\eta^2} - \frac{\mathcal{F}}{Q}\sin(\Theta_0) ,$$

where

$$c^2 = \frac{\mu - 3q^2}{\mu - q^2} .$$

By rescaling the variables as follows:

$$\tau \to \tau\sqrt{\frac{\mathcal{F}}{Q}} , \quad \eta \to \eta\, c\sqrt{\frac{\mathcal{F}}{Q}} , \tag{14}$$

the phase equation takes the standard form of the Sine–Gordon equation:

$$\frac{\partial^2\Theta_0}{\partial\tau^2} = \frac{\partial^2\Theta_0}{\partial\eta^2} - \sin(\Theta_0) . \tag{15}$$

This equation is known to be integrable via the inverse scattering transform [42]. In the present context, it is sufficient to note that Eq. (15) admits a one-parameter family of soliton solutions that may be written as follows:

$$\Theta_0(\eta,\ \tau;\ \beta) = \pm 4\tan^{-1}\left[\exp\left(\frac{\eta - \beta\tau}{\sqrt{1-\beta^2}}\right)\right] , \tag{16}$$

the parameter β being an arbitrary propagation velocity in the range $|\beta| \le 1$. As shown in the sketches of Fig. 5, such kink or antikink solutions correspond to $\pm 2\pi$ phase jumps which travel along the positive or negative η axis. If one reconstructs the total interface deformation by including the carrier wave of wavenumber q, the $\pm 2\pi$ phase solitons are seen to be associated with local contractions or dilatations of the primary periodic structures that propagate along the interface.

The existence of propagating phase solitons has only been demonstrated in the phase dynamics approximation based on the asymptotic scheme (13). To confirm that the same features prevail in the full amplitude equation, direct numerical simulations of

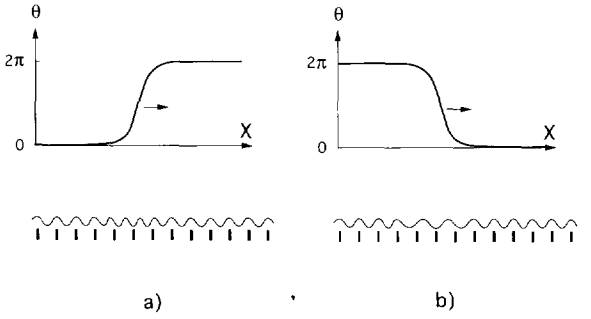

Fig. 5. Sine–Gordon solitons and corresponding interface deformations. Black vertical segments indicate the periodicity of forcing. (a) $+2\pi$ soliton; (b) -2π soliton.

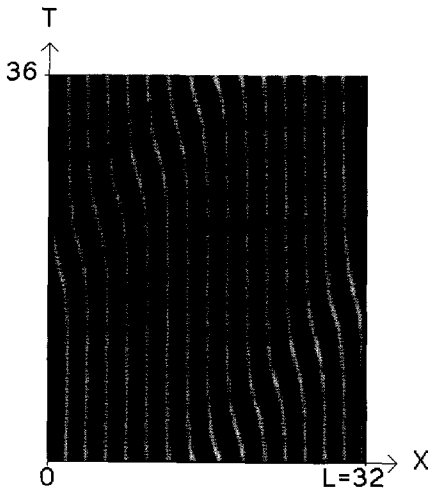

Fig. 6. Spatio-temporal $X-T$ diagram of the elevation of the interface, calculated from a direct simulation of the Klein–Gordon equation, with a -2π Sine–Gordon soliton as initial condition (see Section 3). $\mu = 3$, $\delta x = 0.4$, $\delta t = 0.012$, $q = 2\pi/L$, $L = 32$, $F = 0.03$, $\beta = 0.95$. The carrier wave at $k_c = 28\pi/L$ has been reintroduced to reconstruct the total elevation.

the Klein–Gordon equation (5) have been carried out with the exact form (16) of the soliton chosen as initial phase distortion for the periodic pattern. As seen on the spatio-temporal diagram of the interface deformation on Fig. 6, a dilatation soliton is produced and it travels along the X axis without any noticeable deformation. Thus the phase dynamics analysis is fully corroborated by direct integration of the Klein–Gordon evolution model.

There remains to determine whether the phase soliton solutions (16) are stable or unstable within the restricted one-dimensional setting adopted in the present

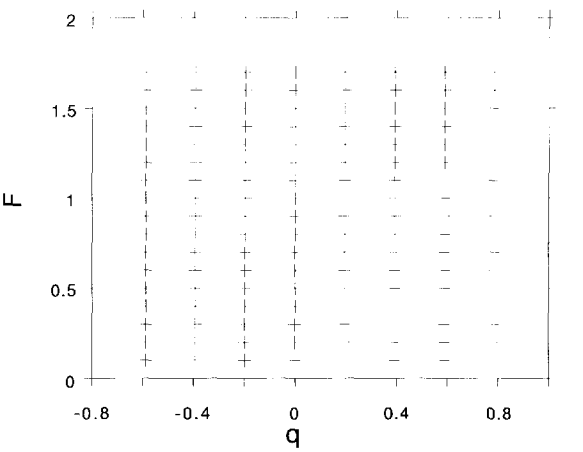

Fig. 7. Stability diagram for a -2π Klein–Gordon soliton in the forcing wavenumber q-forcing amplitude F plane. $\mu = 3$, $\delta x = 0.4$, $\beta = 0.94$. $-$: stable solitons (no detectable deformation within the first 8000 time iterations); $+$: unstable solitons.

investigation. In the notation of Eq. (5) phase soliton solutions depend on all three parameters μ, q and F and on the velocity parameter β. In order to determine their stability numerical simulations of Eq. (5) are undertaken at $\mu = 3$ and $\beta = 0.94$ for different pairs of values of q and F with the same type of soliton initial conditions as before. The stability properties of solitons with a -2π phase jump are summarized on Fig. 7, the $+$ and $-$ symbols indicating stable and unstable solitons respectively. A soliton is said to be stable if numerical noise leaves the interface deformations unchanged over the time interval $T = 180$. It is not necessary to add any external noise and the results obtained in this manner are not modified if one increases the duration of the run above $T = 180$.

Negative phase jumps are seen to be all unstable for negative values of q. In such conditions, spatial forcing of wavenumber $k_c+q < k_c$ uniformly dilates the periodic pattern below its natural wavenumber k_c. The creation at time $t = 0$ of a -2π phase soliton produces an additional local enhancement of this dilatation which the system is incapable of accommodating. As shown on Fig. 8, a new structure is created which annihilates the initially imposed (-2π) phase jump. This nucleation process takes the form of a spatio-temporal dislocation in the $X-T$ plane. Such a behavior may be interpreted in terms of the primary instability mecha-

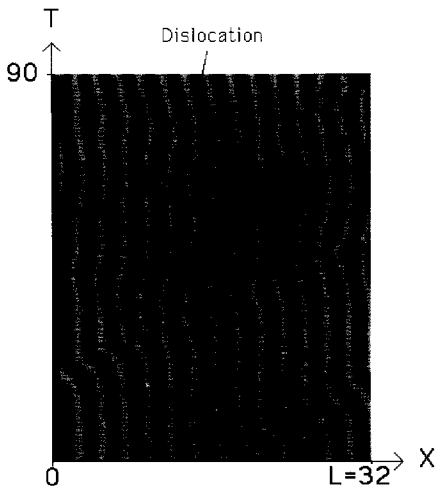

Fig. 8. Spatio-temporal $X-T$ diagram of the elevation of the interface, calculated from a direct simulation of the Klein–Gordon equation, with a -2π unstable Sine–Gordon soliton as initial condition (see Section 3). $\mu = 2.5$, $\delta x = 0.4$, $\delta t = 0.03$, $q = -2\pi/L$, $L = 32$, $F = 0.03$, $\beta = 0.95$. The carrier wave at $k_c = 28\pi/L$ has been reintroduced to reconstruct the total elevation.

nism: stable phase jumps are those which tend to bring the periodic pattern closer to its "natural" periodicity k_c. By contrast, when $q > 0$, spatial forcing at $k_c + q$ compresses the structures above the wavenumber k_c. -2π dilatational phase jumps then have a stabilizing influence on the pattern since they locally decrease the wavenumber closer to k_c. However, not all -2π phase jumps are stable: when the forcing level F becomes too high, the interface is strongly constrained to follow the imposed wavenumber $k_c + q$ and again the phase jump is annihilated eventhough it produces a local dilatation.

The stability diagram of 2π compressive phase jumps is deduced from Fig. 7 by a trivial reflection around the F axis and the same qualitative arguments are naturally applicable.

The above reasoning strongly indicates that propagative phase solitons result from the competition between the natural instability of wavenumber k_c and external spatial forcing of wavenumber $k_f = k_c + q$. When one mechanism dominates over the other, Sine–Gordon solitons become unstable.

5. Concluding remarks

The main conclusion of the present study can be stated as follows: when spatially periodic forcing is imposed to the vortex sheet separating two counter-moving streams of immiscible fluids, traveling phase solitons are produced along the interface in the form of local compressions or dilatations of the basic pattern. The propagative nature of the solitons is intimately related to the conservative character of the Kelvin–Helmholtz instability.

As stated in the introduction, phase solitons have also been observed in earlier spatially forced tilting tank experiments [21]: when the forcing wavenumber k_f slightly exceeds the natural wavenumber k_n of the Kelvin–Helmholtz instability, the interface experiences a transition to an incommensurate state which is first signaled by the appearance of a single phase soliton, in qualitative agreement with the present theory. However, experimental observations differ from the predictions of the Sine–Gordon model in two important respects. First, the observed phase jumps are stationary over the duration of a run and it has not been possible to ascribe to them a finite propagation velocity with any reasonable degree of confidence. This discrepancy is likely to be due to the highly transient nature of the experiment which is too brief to capture the slow evolution times typical of phase dynamics. Secondly, -2π phase jumps are created when $k_f > k_n$ but we have not succeeded in producing $+2\pi$ phase jumps when $k_f < k_n$, although the theoretical model does not introduce any bias between $+2\pi$ and -2π solitons. Finally, it should be emphasized that the experiments are performed in the accelerating mode whereby the tube is kept tilted at a finite angle until the end of the run. The resulting basic flow is therefore accelerating with a velocity difference across the interface that increases linearly with time. Consequently, the experimentally generated basic flow does not remain in the vicinity of threshold, in a regime where the weakly nonlinear analysis developed here is likely to be directly applicable.

To overcome the latter difficulty, experiments have recently been undertaken [38] in the constant shear mode where the tank is returned to its horizontal posi-

tion beyond an initial accelerating phase. The velocity difference is therefore approximately constant and it can be kept close to the threshold value over the duration of the run. It is then found that the presence of thin diffusive layers on either side of the interface drastically alters the nature of the *primary* instability. The stationary Kelvin–Helmholtz mode predicted by the vortex sheet model is replaced close to onset by traveling Holmboe instability waves. The vortex sheet analysis is consequently no longer valid as shown in [38].

Acknowledgements

We wish to thank S. Le Dizes for many helpful comments and discussions.

LadHyX is part of URA 317, Centre National de la Recherche Scientifique (CNRS). The financial support of the Direction des Recherches, Etudes et Techniques (DRET) of the French Ministry of Defense under Grant #90-040 and of the Direction des laboratoires (Ecole Polytechnique) is gratefully acknowledged.

Appendix A. Derivation of the amplitude evolution equations

The characteristics of the basic flow sketched on Fig. 1 have been defined at the beginning of Section 2. The perturbed inviscid two- dimensional flow is irrotational and the pressure field in each layer can be expressed as follows:

$$\boldsymbol{v}_i^* = U_i^* \boldsymbol{e}_x + \nabla \phi_i^* ,$$

$$P_i^* = -\rho_i^* g^* y^* + p_i^* ,$$

where $i = 1$ (respectively $i = 2$) refer to the lower (respectively upper) layer, ϕ_i^* is the perturbation velocity potential, p_i^* the perturbation pressure and $\boldsymbol{e}_x$ the unit vector along the streamwise direction.

All variables are made nondimensional with respect to the density scale $\rho_1^* + \rho_2^*$, the capillary length scale L^* and the velocity scale V^* introduced in Section 2. In terms of nondimensional unstarred field quantities, Laplace's equation for the perturbation velocity potentials ϕ_i reads

$$\frac{\partial^2 \phi_i}{\partial x^2} + \frac{\partial^2 \phi_i}{\partial y^2} = 0 , \tag{A.1a}$$

the velocity field and perturbation pressure being related to the perturbation potential through the expressions

$$\boldsymbol{v}_i = U_i \boldsymbol{e}_x + \nabla \phi_i , \tag{A.1b}$$

$$p_i = -\left(\frac{\partial}{\partial t} + \boldsymbol{v}_i \cdot \nabla \right) \phi_i . \tag{A.1c}$$

At the deformed interface $y = \xi(x, t)$, one must satisfy the continuity of particle displacement conditions

$$v_{i_y}\big|_{y=\xi} = \left(\frac{\partial}{\partial t} + \boldsymbol{v}_i \cdot \nabla \right) \xi , \quad i = 1, 2 , \tag{A.1d}$$

together with the pressure jump condition

$$\rho_2 \, p_2\big|_{y=\xi} - \rho_1 \, p_1\big|_{y=\xi} = -\xi + \left. \frac{\partial^2 \xi}{\partial x^2} \right|_{y=\xi} \left[1 + \left(\left. \frac{\partial \xi}{\partial x} \right|_{y=\xi} \right)^2 \right]^{-3/2} . \tag{A.1e}$$

Finally, the impermeability conditions at the upper and lower boundaries take the form

$$\left.\frac{\partial \phi_2}{\partial y}\right|_{y=+h} = 0\,, \tag{A.1f}$$

$$\boldsymbol{v}_1 \cdot \boldsymbol{n}|_{y=-h+2f\cos(k_f x)} = 0\,, \tag{A.1g}$$

where $\boldsymbol{n}$ is the unit vector normal to the modulated lower wall.

Following classical weakly nonlinear analysis, system (A.1) is solved in the vicinity of the threshold of instability defined by the critical velocities U_{i_c}, the critical wavenumber k_c and imaginary critical growth rate σ_c. Exact expressions for these quantities will be given later when we examine the first- order solutions. Supercriticality parameters Δ_i are introduced such that

$$U_i = U_{i_c} + \varepsilon^2 \Delta_i\,,$$

where $\varepsilon \ll 1$ is a small parameter. As discussed in Section 2, slow space and time variables $(X,T) = \varepsilon(x,t)$ are defined and all dependent variables are expanded in the form

$$\{\phi_i, p_i, \xi\} = \varepsilon \left\{\phi_i^{(1)}, p_i^{(1)}, \xi^{(1)}\right\} + \varepsilon^2 \left\{\phi_i^{(2)}, p_i^{(2)}, \xi^{(2)}\right\} + \varepsilon^3 \left\{\phi_i^{(3)}, p_i^{(3)}, \xi^{(3)}\right\} + \cdots\,, \tag{A.2}$$

where $\left\{\phi_i^{(j)}, p_i^{(j)}, \xi^{(j)}\right\}$ are all of order unity. Finally, the modulated lower wall forces the flow at a nearly resonant wavenumber $k_f = k_c + q\varepsilon$ with an $\mathcal{O}(\varepsilon^3)$ amplitude so that its shape is given by

$$y = -h + 2\varepsilon^3 F_0 \cos\left((k_c + q\varepsilon)x\right)\,.$$

The misfit parameter q and the normalized forcing amplitude F_0 are both $\mathcal{O}(1)$.

By substituting expansion (A.2) into the governing equations (A.1) one obtains a sequence of perturbation problems as outlined below.

Order ε problem:

$$\frac{\partial^2 \phi_i^{(1)}}{\partial x^2} + \frac{\partial^2 \phi_i^{(1)}}{\partial y^2} = 0\,,$$

$$p_i^{(1)} + \left(\frac{\partial}{\partial t} + U_{i_c}\frac{\partial}{\partial x}\right)\phi_i^{(1)} = 0\,,$$

$$\left.\frac{\partial \phi_i^{(1)}}{\partial y}\right|_{y=0} - \left(\frac{\partial}{\partial t} + U_{i_c}\frac{\partial}{\partial x}\right)\xi^{(1)} = 0\,,$$

$$\rho_2\, p_2^{(1)}\Big|_{y=0} - \rho_1\, p_1^{(1)}\Big|_{y=0} + \xi^{(1)} - \frac{\partial^2 \xi^{(1)}}{\partial x^2} = 0\,,$$

$$\left.\frac{\partial \phi_2^{(1)}}{\partial y}\right|_{y=h} = \left.\frac{\partial \phi_1^{(1)}}{\partial y}\right|_{y=-h} = 0\,.$$

Solutions of wavenumber k_c and imaginary growth rate σ_c are sought in the form:

$$\xi^{(1)} = A^{(1)}(X,T)\exp(\sigma_c t + ik_c x) + \text{c.c.}\,,$$

$$\phi_i^{(1)} = (B_i^{(1)}(X,T)e^{-k_c y} + C_i^{(1)}(X,T)e^{k_c y})\exp(\sigma_c t + ik_c x) + \text{c.c.}\,,$$

where $A^{(1)}(X,T)$, $B_i^{(1)}(X,T)$ and $C_i^{(1)}(X,T)$ are, at this stage, unknown functions of the slow variables X and T.

By substitution of the assumed solutions into the interface and boundary conditions above, one is led to the following homogeneous linear system:

$$\begin{pmatrix} \frac{a_1}{k_c} & -1 & 1 & 0 & 0 \\ 0 & e^{k_c h} & -e^{-k_c h} & 0 & 0 \\ \frac{a_2}{k_c} & 0 & 0 & -1 & 1 \\ 0 & 0 & 0 & e^{-k_c h} & -e^{k_c h} \\ (1+k_c^2) & -\rho_1 a_1 & -\rho_1 a_1 & \rho_2 a_2 & \rho_2 a_2 \end{pmatrix} \begin{pmatrix} A^{(1)} \\ B_1^{(1)} \\ C_1^{(1)} \\ B_2^{(1)} \\ C_2^{(1)} \end{pmatrix} \equiv \mathbf{M} \begin{pmatrix} A^{(1)} \\ B_1^{(1)} \\ C_1^{(1)} \\ B_2^{(1)} \\ C_2^{(1)} \end{pmatrix} = 0 , \tag{A.3}$$

where $a_i = -(\sigma_c + ik_c U_{i_c})$. In order to obtain a nontrivial solution, one must set the determinant of the matrix $\mathbf{M}$ equal to zero, which yields the dispersion relation:

$$D(\sigma_c,\ k_c,\ U_{1_c},\ U_{2_c}) = 0 ,$$

where

$$D(\sigma,\ k,\ U_1,\ U_2) \equiv -\left[\sigma + ik(\rho_1 U_1 + \rho_2 U_2)\right]^2 + \rho_1\rho_2 k^2 (\Delta U)^2 - (k + k^3)\tanh(kh) ,$$

with $\Delta U \equiv U_2 - U_1$. The interface response will resonate with the stationary boundary only if one imposes the zero critical phase velocity condition

$$-\sigma_c / ik_c \equiv \rho_1 U_{1_c} + \rho_2 U_{2_c} = 0 . \tag{A.4}$$

The other critical parameters U_{1_c}, U_{2_c} and k_c are then completely defined by the conditions

$$D_\sigma = D_k = 0 , \tag{A.5}$$

which yields the critical velocity difference

$$(\Delta U_c)^2 \equiv \left(U_{2_c} - U_{1_c}\right)^2 = \frac{1}{\rho_1\rho_2}\left(k_c + \frac{1}{k_c}\right)\tanh(k_c h) ,$$

with k_c satisfying:

$$\frac{\partial}{\partial k}\left[\left(k + \frac{1}{k}\right)\tanh(kh)\right]\Big|_{k=k_c} = 0 .$$

The above relation gives a non-zero value of k_c only if the scaled height h satisfies $h > \sqrt{3}$. This assumption is made in the sequel. Under these conditions, system (A.3) may be solved for the functions $B_i^{(1)}(X,T)$ and $C_i^{(1)}(X,T)$ in terms of $A^{(1)}(X,T)$. One obtains:

$$B_1^{(1)}(X,T) = \frac{a_1 A^{(1)}(X,T)}{k_c(1 - e^{2k_c h})} , \quad B_2^{(1)}(X,T) = \frac{a_2 A^{(1)}(X,T)}{k_c(1 - e^{-2k_c h})} ,$$

$$C_1^{(1)}(X,T) = \frac{a_1 A^{(1)}(X,T)}{k_c(e^{-2k_c h} - 1)} , \quad C_2^{(1)}(X,T) = \frac{a_2 A^{(1)}(X,T)}{k_c(e^{2k_c h} - 1)} .$$

It should be emphasized that, in contrast to the case of infinitely deep fluid layers [23], the $\mathcal{O}(\varepsilon)$ solution is not solely composed of a linearised neutral component of wavenumber k_c. In order to satisfy all the compatibility conditions appearing in higher-order problems, it is necessary, at this stage, to add in each layer an arbitrary streamwise velocity in the form of unknown real amplitude potentials $\mathcal{M}_i^{(1)}(X,T)$, $i=1,2$. These complementary solutions of the linearised problem at *zero wavenumber* are related to the Galilean invariance of the problem, as discussed in Section 2. Thus the total $\mathcal{O}(\varepsilon)$ perturbation is taken to be:

$$\xi^{(1)} = A^{(1)}(X,T)\exp(\sigma_c t + ik_c x) + \text{c.c.},$$
$$\phi_i^{(1)} = \mathcal{M}_i^{(1)}(X,T) + \left[(B_i^{(1)}(X,T)e^{-k_c y} + C_i^{(1)}(X,T)e^{k_c y})\exp(\sigma_c t + ik_c x) + \text{c.c.}\right],$$
$$p_i^{(1)} = -ik_c U_{i_c}(B_i^{(1)}(X,T)e^{-k_c y} + C_i^{(1)}(X,T)e^{k_c y})\exp(\sigma_c t + ik_c x) + \text{c.c.},$$

where $\mathcal{M}_i^{(1)}(X,T)$, $i=1,2$, are unknown mean potential functions in the lower and upper fluid respectively.

Order ε^2 problem:

$$\frac{\partial^2\phi_i^{(2)}}{\partial x^2} + \frac{\partial^2\phi_i^{(2)}}{\partial y^2} = -\frac{\partial^2\phi_i^{(1)}}{\partial x \partial X}, \tag{A.6}$$

$$p_i^{(2)} + \left(\frac{\partial}{\partial t} + U_{i_c}\frac{\partial}{\partial x}\right)\phi_i^{(2)} = -\left(\frac{\partial}{\partial T} + U_{i_c}\frac{\partial}{\partial X}\right)\phi_i^{(1)} - \frac{1}{2}\left[\left(\frac{\partial\phi_i^{(1)}}{\partial x}\right)^2 + \left(\frac{\partial\phi_i^{(1)}}{\partial y}\right)^2\right],$$

$$\left.\frac{\partial\phi_i^{(2)}}{\partial y}\right|_{y=0} - \left(\frac{\partial}{\partial t} + U_{i_c}\frac{\partial}{\partial x}\right)\xi^{(2)} = \left(\frac{\partial}{\partial T} + U_{i_c}\frac{\partial}{\partial X}\right)\xi^{(1)} + \frac{\partial}{\partial x}\left[\xi^{(1)}\left.\frac{\partial\phi_i^{(1)}}{\partial x}\right|_{y=0}\right],$$

$$\rho_2\, p_2^{(2)}\Big|_{y=0} - \rho_1\, p_1^{(2)}\Big|_{y=0} + \xi^{(2)} - \frac{\partial^2\xi^{(2)}}{\partial x^2} = -\xi^{(1)}\left(\rho_2\left.\frac{\partial p_2^{(1)}}{\partial y}\right|_{y=0} - \rho_1\left.\frac{\partial p_1^{(1)}}{\partial y}\right|_{y=0}\right) + 2\frac{\partial^2\xi^{(1)}}{\partial x\partial X}, \tag{A.7}$$

$$\left.\frac{\partial\phi_2^{(2)}}{\partial y}\right|_{y=h} = 0, \quad \left.\frac{\partial\phi_1^{(2)}}{\partial y}\right|_{y=-h} = 0.$$

The forcing terms on the right-hand side of the above system generate mean, fundamental and second harmonic components. It is convenient to examine the fundamental contribution of wavenumber k_c denoted by the letter "f" separately and to seek a *partial* solution of the form

$$f\xi^{(2)} = A^{(2)}(X,T)\exp(ik_c x) + \text{c.c.},$$
$$f\phi_i^{(2)} = \left[\left(B_i^{(2)}(X,T) + F_i^{(2)}(X,T)y\right)e^{-k_c y} + \left(C_i^{(2)}(X,T) + H_i^{(2)}(X,T)y\right)e^{k_c y}\right]\exp(ik_c x) + \text{c.c.}.$$

The mass conservation equation (A.6) implies the following relations:

$$F_i^{(2)}(X,T) = i\frac{\partial B_i^{(1)}}{\partial X}(X,T), \quad H_i^{(2)}(X,T) = -i\frac{\partial C_i^{(1)}}{\partial X}(X,T).$$

As a consequence of the interface and boundary conditions, the remaining unknown functions must then satisfy the linear system:

$$\mathbf{M}\begin{pmatrix} A^{(2)} \\ B_1^{(2)} \\ C_1^{(2)} \\ B_2^{(2)} \\ C_2^{(2)} \end{pmatrix} = \begin{pmatrix} z_1^{(2)} \\ z_2^{(2)} \\ z_3^{(2)} \\ z_4^{(2)} \\ z_5^{(2)} \end{pmatrix},$$

where

$$z_1^{(2)} = \frac{1}{k_c}\left(\frac{\partial}{\partial T} + U_{1_c}\frac{\partial}{\partial X}\right)A^{(1)} - \frac{i}{k_c}\frac{\partial B_1^{(1)}}{\partial X} + \frac{i}{k_c}\frac{\partial C_1^{(1)}}{\partial X},$$

$$z_2^{(2)} = e^{k_c h}\left(k_c + \frac{1}{k_c}\right)i\frac{\partial B_1^{(1)}}{\partial X} + e^{-k_c h}\left(k_c - \frac{1}{k_c}\right)i\frac{\partial C_1^{(1)}}{\partial X},$$

$$z_3^{(2)} = \frac{1}{k_c}\left(\frac{\partial}{\partial T} + U_{2_c}\frac{\partial}{\partial X}\right)A^{(1)} - \frac{i}{k_c}\frac{\partial B_2^{(1)}}{\partial X} + \frac{i}{k_c}\frac{\partial C_2^{(1)}}{\partial X},$$

$$z_4^{(2)} = e^{-k_c h}\left(\frac{1}{k_c} - k_c\right)i\frac{\partial B_2^{(1)}}{\partial X} - e^{k_c h}\left(k_c + \frac{1}{k_c}\right)i\frac{\partial C_2^{(1)}}{\partial X},$$

$$z_5^{(2)} = 2ik_c\frac{\partial A^{(1)}}{\partial X} + \rho_2\left(\frac{\partial}{\partial T} + U_{2_c}\frac{\partial}{\partial X}\right)\left(B_2^{(1)} + C_2^{(1)}\right) - \rho_1\left(\frac{\partial}{\partial T} + U_{1_c}\frac{\partial}{\partial X}\right)\left(B_1^{(1)} + C_1^{(1)}\right).$$

In order for this system to admit a nontrivial solution, the vector $z^{(2)}$ must be orthogonal to the kernel of the adjoint matrix M generated by the vector K such that

$$K^{\perp} = \left(\frac{\rho_1\overline{a_1}}{\tanh(k_c h)}, \frac{\rho_1\overline{a_1}}{\sinh(k_c h)}, \frac{\rho_2\overline{a_2}}{\tanh(k_c h)}, \frac{\rho_2\overline{a_2}}{\sinh(k_c h)}, 1\right),$$

where a bar denotes the complex conjugate. The orthogonality condition $\sum_{i=1}^{5}\overline{K_i}z_i^{(2)} = 0$ then leads to the following amplitude equation for $A^{(1)}(X,T)$:

$$iD_\sigma\frac{\partial A^{(1)}}{\partial T} + D_k\frac{\partial A^{(1)}}{\partial X} = 0.$$

The above equation reflects the local properties of the dispersion relation in the vicinity of the critical wavenumber k_c. According to the conditions (A.5), the derivative coefficients D_σ and D_k vanish at critical. The orthogonality condition is therefore trivially satisfied at this order. Without loss of generality, the amplitude function $A^{(2)}$ may be set equal to zero.

The fundamental component at order ε^2 is then found to take the final form:

$$f\xi^{(2)} = 0,$$

$$f\phi_i^{(2)} = \left[\left(B_i^{(2)} + F_i^{(2)}y\right)e^{-k_c y} + \left(C_i^{(2)} + H_i^{(2)}y\right)e^{k_c y}\right]\exp(ik_c x) + \text{c.c.},$$

$$fp_i^{(2)} = -ik_c U_{i_c}\left[\left(B_i^{(2)} + F_i^{(2)}y - \frac{\partial B_i^{(1)}}{\partial T} - U_{i_c}\frac{\partial B_i^{(1)}}{\partial X}\right)e^{-k_c y} + \left(C_i^{(2)} + H_i^{(2)}y - \frac{\partial C_i^{(1)}}{\partial T} - U_{i_c}\frac{\partial C_i^{(1)}}{\partial X}\right)e^{k_c y}\right]exp(ik_c x) + \text{c.c.},$$

where

$$B_1^{(2)} = \frac{\partial A^{(1)}}{\partial T}\left(\frac{e^{-k_c h}}{2k_c \sinh(k_c h)}\right) - \frac{\partial A^{(1)}}{\partial X}\left(\frac{U_{1_c} h}{2\sinh^2(k_c h)}\right),$$

$$B_2^{(2)} = -\frac{\partial A^{(1)}}{\partial T}\left(\frac{e^{k_c h}}{2k_c \sinh(k_c h)}\right) + \frac{\partial A^{(1)}}{\partial X}\left(\frac{U_{2_c} h}{2\sinh^2(k_c h)}\right),$$

$$C_1^{(2)} = \frac{\partial A^{(1)}}{\partial T}\left(\frac{e^{k_c h}}{2k_c \sinh(k_c h)}\right) - \frac{\partial A^{(1)}}{\partial X}\left(\frac{U_{1_c} h}{2\sinh^2(k_c h)}\right),$$

$$C_2^{(2)} = -\frac{\partial A^{(1)}}{\partial T}\left(\frac{e^{-k_c h}}{2k_c \sinh(k_c h)}\right) + \frac{\partial A^{(1)}}{\partial X}\left(\frac{U_{2_c} h}{2\sinh^2(k_c h)}\right).$$

The second harmonic component of wavenumber $2k_c$ identified by the letter "s" may be calculated without difficulty and it is found to be

$$s\xi^{(2)} = sA^{(2)} \exp(2ik_c x) + \text{c.c.},$$

$$s\phi_i^{(2)} = \left[sB_i^{(2)} e^{-2k_c y} + sC_i^{(2)} e^{2k_c y}\right] \exp(2ik_c x) + \text{c.c.},$$

$$sp_i^{(2)} = -2ik_c U_{i_c}\left(sB_i^{(2)} e^{-2k_c y} + sC_i^{(2)} e^{2k_c y}\right) \exp(2ik_c x) + \text{c.c.},$$

where

$$sA^{(2)} = \Gamma\left(A^{(1)}\right)^2,$$

$$sB_1^{(2)} = -\frac{ik_c U_{1_c}\left(A^{(1)}\right)^2}{e^{4k_c h} - 1}\left(\frac{1}{\tanh(k_c h)} - \frac{\Gamma}{k_c}\right),$$

$$sB_2^{(2)} = \frac{ik_c U_{2_c}\left(A^{(1)}\right)^2}{e^{-4k_c h} - 1}\left(\frac{1}{\tanh(k_c h)} + \frac{\Gamma}{k_c}\right),$$

$$sC_1^{(2)} = \frac{ik_c U_{1_c}\left(A^{(1)}\right)^2}{e^{-4k_c h} - 1}\left(\frac{1}{\tanh(k_c h)} - \frac{\Gamma}{k_c}\right),$$

$$sC_2^{(2)} = -\frac{ik_c U_{2_c}\left(A^{(1)}\right)^2}{e^{4k_c h} - 1}\left(\frac{1}{\tanh(k_c h)} + \frac{\Gamma}{k_c}\right).$$

The constant Γ is defined as

$$\Gamma \equiv k_c^2\left(1 - \frac{2}{\tanh(k_c h)}\right)\frac{\rho_2 U_{2_c}^2 - \rho_1 U_{1_c}^2}{\left(1 + k_c^2\right)\tanh^2(k_c h) - 3k_c^2}.$$

Finally the mean component identified by the letter "m" is given by

$$m\xi^{(2)} = \mathcal{H}^{(2)}(X,T),$$

$$m\phi_i^{(2)} = \mathcal{M}_i^{(2)}(X,T),$$

$$mp_i^{(2)} = -\left(\frac{\partial}{\partial T} + U_{i_c}\frac{\partial}{\partial X}\right)\mathcal{M}_i^{(1)} - 2k_c^2\left(\left|B_i^{(1)}\right|^2 e^{-2k_c y} + \left|C_i^{(1)}\right|^2 e^{2k_c y}\right).$$

In the $\mathcal{O}(\varepsilon^2)$ solution, the mean component at zero wavenumber is seen to involve three unknown real amplitude functions: the mean perturbation potentials in each layer $\mathcal{M}_i^{(2)}(X,T)$, $i = 1,2$ and the mean elevation of the interface $\mathcal{H}^{(2)}(X,T)$. These functions are the counterparts of the mean components[2] introduced at $\mathcal{O}(\varepsilon)$. Upon enforcing the pressure jump condition (A.7) at zero wavenumber one obtains the following evolution equation for the mean fields:

$$\mathcal{H}^{(2)} + \rho_1 \left(\frac{\partial}{\partial T} + U_{1_c}\frac{\partial}{\partial X}\right)\mathcal{M}_1^{(1)} - \rho_2 \left(\frac{\partial}{\partial T} + U_{2_c}\frac{\partial}{\partial X}\right)\mathcal{M}_2^{(1)} = S|A|^2 , \tag{A.8}$$

with the real constant S given by

$$S = \frac{k_c^2\left(\rho_2 U_{2_c}^2 - \rho_1 U_{1_c}^2\right)}{\sinh^2(k_c h)} . \tag{A.9}$$

The total solution at $\mathcal{O}(\varepsilon^2)$ is given by

$$\xi^{(2)} = m\xi^{(2)} + f\xi^{(2)} + s\xi^{(2)} ,$$
$$\phi_i^{(2)} = m\phi_i^{(2)} + f\phi_i^{(2)} + s\phi_i^{(2)} ,$$
$$p_i^{(2)} = mp_i^{(2)} + fp_i^{(2)} + sp_i^{(2)} .$$

Order ε^3 problem:

$$\frac{\partial^2\phi_i^{(3)}}{\partial x^2} + \frac{\partial^2\phi_i^{(3)}}{\partial y^2} = -2\frac{\partial^2\phi_i^{(2)}}{\partial x\partial X} - \frac{\partial^2\phi_i^{(1)}}{\partial X^2} ,$$

$$p_i^{(3)} + \left(\frac{\partial}{\partial t} + U_{i_c}\frac{\partial}{\partial x}\right)\phi_i^{(3)} = -\left(\frac{\partial}{\partial T} + U_{i_c}\frac{\partial}{\partial X}\right)\phi_i^{(2)} - \nabla\phi_i^{(1)}.\nabla\phi_i^{(2)} - \frac{\partial\phi_i^{(1)}}{\partial x}\frac{\partial\phi_i^{(1)}}{\partial X} - \Delta_i\frac{\partial\phi_i^{(1)}}{\partial x} ,$$

$$\left.\frac{\partial\phi_i^{(3)}}{\partial y}\right|_{y=0} - \left(\frac{\partial}{\partial t} + U_{i_c}\frac{\partial}{\partial x}\right)\xi^{(3)} = \left(\frac{\partial}{\partial T} + U_{i_c}\frac{\partial}{\partial X}\right)\xi^{(2)} + \frac{1}{2}\frac{\partial}{\partial x}\left[\left(\xi^{(1)}\right)^2\left.\frac{\partial^2\phi_i^{(1)}}{\partial x\partial y}\right|_{y=0}\right]$$
$$+\frac{\partial}{\partial x}\left[\xi^{(1)}\left.\frac{\partial\phi_i^{(2)}}{\partial x}\right|_{y=0}\right] + \frac{\partial}{\partial x}\left[\xi^{(2)}\left.\frac{\partial\phi_i^{(1)}}{\partial x}\right|_{y=0}\right] + \left.\frac{\partial\xi^{(1)}}{\partial X}\frac{\partial\phi_i^{(1)}}{\partial x}\right|_{y=0} + \left.\frac{\partial\xi^{(1)}}{\partial x}\frac{\partial\phi_i^{(1)}}{\partial X}\right|_{y=0} + \Delta_i\frac{\partial\xi^{(1)}}{\partial x} , \tag{A.10a}$$

$$\rho_2\left.p_2^{(3)}\right|_{y=0} - \rho_1\left.p_1^{(3)}\right|_{y=0} + \xi^{(3)} - \frac{\partial^2\xi^{(3)}}{\partial x^2} = 2\frac{\partial^2\xi^{(2)}}{\partial x\partial X} + \frac{\partial^2\xi^{(1)}}{\partial X^2} - \xi^{(1)}\left(\rho_2\left.\frac{\partial p_2^{(2)}}{\partial y}\right|_{y=0} - \rho_1\left.\frac{\partial p_1^{(2)}}{\partial y}\right|_{y=0}\right)$$
$$-\frac{3}{2}\frac{\partial^2\xi^{(1)}}{\partial x^2}\left(\frac{\partial\xi^{(1)}}{\partial x}\right)^2 - \xi^{(2)}\left(\rho_2\left.\frac{\partial p_2^{(1)}}{\partial y}\right|_{y=0} - \rho_1\left.\frac{\partial p_1^{(1)}}{\partial y}\right|_{y=0}\right) - \frac{\left(\xi^{(1)}\right)^2}{2}\left(\rho_2\left.\frac{\partial^2 p_2^{(1)}}{\partial y^2}\right|_{y=0} - \rho_1\left.\frac{\partial^2 p_1^{(1)}}{\partial y^2}\right|_{y=0}\right) , \tag{A.10b}$$

$$\left.\frac{\partial\phi_1^{(3)}}{\partial y}\right|_{y=-h} = iU_1F_0k_c\exp\left(i\left(k_cx + qX\right)\right) + \text{c.c.} , \tag{A.11}$$

[2] Note, however that we had then omitted to include a mean elevation function $\mathcal{H}^{(1)}(X,T)$. If it had been introduced, we would have found from the $\mathcal{O}(\varepsilon)$ pressure condition that $\mathcal{H}^{(1)}(X,T) \equiv 0$.

$$\left.\frac{\partial \phi_2^{(3)}}{\partial y}\right|_{y=h} = 0 . \tag{A.12}$$

It is only necessary to consider at this stage the mean and fundamental contributions.

The fundamental component at wavenumber k_c is of the form

$$\xi^{(3)} = A^{(3)} \exp(ik_c x) + \text{c.c.} ,$$

$$\phi_i^{(3)} = \left[\left(B_i^{(3)} + F_i^{(3)} y + G_i^{(3)} y^2\right) e^{-k_c y} + \left(C_i^{(3)} + H_i^{(3)} y + I_i^{(3)} y^2\right) e^{k_c y}\right] \exp(ik_c x) + \text{c.c.} ,$$

where

$$F_i^{(3)}(X,T) = i\frac{\partial B_i^{(2)}}{\partial X}(X,T) , \quad G_i^{(3)}(X,T) = -\frac{1}{2}\frac{\partial^2 B_i^{(1)}}{\partial X^2}(X,T) ,$$

$$H_i^{(3)}(X,T) = -i\frac{\partial C_i^{(2)}}{\partial X}(X,T) , \; I_i^{(3)}(X,T) = -\frac{1}{2}\frac{\partial^2 C_i^{(1)}}{\partial X^2}(X,T) .$$

The remaining unknown functions satisfy the linear system

$$\mathbf{M}\begin{pmatrix} A^{(3)} \\ B_1^{(3)} \\ C_1^{(3)} \\ B_2^{(3)} \\ C_2^{(3)} \end{pmatrix} = \begin{pmatrix} z_1^{(3)} \\ z_2^{(3)} \\ z_3^{(3)} \\ z_4^{(3)} \\ z_5^{(3)} \end{pmatrix} ,$$

where the forcing terms are given by

$$\begin{aligned} z_1^{(3)} = & -\frac{i}{k_c}\frac{\partial B_1^{(2)}}{\partial X} + \frac{i}{k_c}\frac{\partial C_1^{(2)}}{\partial X} + iA^{(1)}\Delta_1 - 2k_c\overline{A^{(1)}}\left(sB_1^{(2)} + sC_1^{(2)}\right) + k_c\Gamma A^{(1)^2}\left(\overline{B_1^{(1)}} + \overline{C_1^{(1)}}\right) \\ & + \tfrac{1}{2}k_c^2 A^{(1)^2}\left(-\overline{B_1^{(1)}} + \overline{C_1^{(1)}}\right) - k_c^2\left|A^{(1)}\right|^2\left(-B_1^{(1)} + C_1^{(1)}\right) + iA^{(1)}\frac{\partial \mathcal{M}_1^{(1)}}{\partial X} , \\ z_2^{(3)} = & iU_1 F_0 k_c e^{iqX} + e^{k_c h}\left[i\frac{\partial B_1^{(2)}}{\partial X}\left(\frac{1}{k_c} + h\right) + \frac{\partial^2 B_1^{(1)}}{\partial X^2}\left(\frac{h}{k_c} + \frac{h^2}{2}\right)\right] \\ & + e^{-k_c h}\left[i\frac{\partial C_1^{(2)}}{\partial X}\left(-\frac{1}{k_c} + h\right) + \frac{\partial^2 C_1^{(1)}}{\partial X^2}\left(\frac{h}{k_c} - \frac{h^2}{2}\right)\right] , \\ z_3^{(3)} = & -\frac{i}{k_c}\frac{\partial B_2^{(2)}}{\partial X} + \frac{i}{k_c}\frac{\partial C_2^{(2)}}{\partial X} + iA^{(1)}\Delta_2 - 2k_c\overline{A^{(1)}}\left(sB_2^{(2)} + sC_2^{(2)}\right) + k_c\Gamma(A^{(1)})^2\left(\overline{B_2^{(1)}} + \overline{C_2^{(1)}}\right) \\ & + \tfrac{1}{2}k_c^2(A^{(1)})^2\left(-\overline{B_2^{(1)}} + \overline{C_2^{(1)}}\right) - k_c^2\left|A^{(1)}\right|^2\left(-B_2^{(1)} + C_2^{(1)}\right) iA^{(1)}\frac{\partial \mathcal{M}_2^{(1)}}{\partial X} , \\ z_4^{(3)} = & e^{-k_c h}\left[i\frac{\partial B_2^{(2)}}{\partial X}\left(\frac{1}{k_c} - h\right) + \frac{\partial^2 B_2^{(1)}}{\partial X^2}\left(-\frac{h}{k_c} + \frac{h^2}{2}\right)\right] \\ & + e^{k_c h}\left[-i\frac{\partial C_2^{(2)}}{\partial X}\left(\frac{1}{k_c} + h\right) - \frac{\partial^2 C_2^{(1)}}{\partial X^2}\left(\frac{h}{k_c} + \frac{h^2}{2}\right)\right] , \end{aligned}$$

$$
\begin{aligned}
z_5^{(3)} = {} & \rho_2 \left[\left(\frac{\partial}{\partial T} + U_{2_c} \frac{\partial}{\partial X} \right) \left(B_2^{(2)} + C_2^{(2)} \right) + 4k_c^2 \left(\overline{B_2^{(1)}} s B_2^{(2)} + \overline{C_2^{(1)}} s C_2^{(2)} \right) \right] \\
& - \rho_1 \left[\left(\frac{\partial}{\partial T} + U_{1_c} \frac{\partial}{\partial X} \right) \left(B_1^{(2)} + C_1^{(2)} \right) + 4k_c^2 \left(\overline{B_1^{(1)}} s B_1^{(2)} + \overline{C_1^{(1)}} s C_1^{(2)} \right) \right] \\
& + 4ik_c^2 \overline{A^{(1)}} \left[\rho_2 U_{2_c} \left(-s B_2^{(2)} + s C_2^{(2)} \right) - \rho_1 U_{1_c} \left(-s B_1^{(2)} + s C_1^{(2)} \right) \right] \\
& - 4k_c^3 A^{(1)} \left[\rho_2 \left(\left| B_2^{(1)} \right|^2 - \left| C_2^{(1)} \right|^2 \right) - \rho_1 \left(\left| B_1^{(1)} \right|^2 - \left| C_2^{(1)} \right|^2 \right) \right] \\
& - ik_c^2 s A^{(2)} \left[\rho_2 U_{2_c} \left(\overline{B_2^{(1)}} + \overline{C_2^{(1)}} \right) - \rho_1 U_{1_c} \left(\overline{B_1^{(1)}} + \overline{C_1^{(1)}} \right) \right] \\
& - ik_c^3 \frac{(A^{(1)})^2}{2} \left[\rho_2 U_{2_c} \left(B_2^{(1)} + C_2^{(1)} \right) - \rho_1 U_{1_c} \left(B_1^{(1)} + C_1^{(1)} \right) \right] \\
& + i\rho_2 k_c \left(\Delta_2 + \frac{\partial \mathcal{M}_2^{(1)}}{\partial X} \right) \left(B_2^{(1)} + C_2^{(1)} \right) - i\rho_1 k_c \left(\Delta_1 + \frac{\partial \mathcal{M}_1^{(1)}}{\partial X} \right) \left(B_1^{(1)} + C_1^{(1)} \right) \\
& - ik_c^2 \mathcal{H}^{(2)} \left[\rho_1 U_{1_c} \left(-B_1^{(1)} + C_1^{(1)} \right) - \rho_2 U_{2_c} \left(-B_2^{(1)} + C_2^{(1)} \right) \right] \\
& + \tfrac{3}{2} k_c^4 \left| A^{(1)} \right|^2 A^{(1)} .
\end{aligned}
$$

Upon enforcing the orthogonality condition $\sum_{i=1}^{5} \overline{K_i} z_i^{(3)} = 0$, one is led to the amplitude equation

$$
\begin{aligned}
& -\tfrac{1}{2} D_{\sigma\sigma} \frac{\partial^2 A^{(1)}}{\partial T^2} + \frac{1}{2} D_{kk} \frac{\partial^2 A^{(1)}}{\partial X^2} = (\Delta_2 - \Delta_1) D_{\Delta U} A^{(1)} + N |A^{(1)}|^2 A^{(1)} + F e^{iqx} \\
& + 2k_c^2 \left(\rho_1 U_{1_c} \frac{\partial \mathcal{M}_1^{(1)}}{\partial X} + \rho_2 U_{2_c} \frac{\partial \mathcal{M}_2^{(1)}}{\partial X} \right) A^{(1)} - R \mathcal{H}^{(2)} A^{(1)} .
\end{aligned} \tag{A.13}
$$

where

$$D_{\sigma\sigma} = -2 , \tag{A.14a}$$

$$D_{\Delta U} = 2\rho_1 \rho_2 k_c^2 \Delta U_c , \tag{A.14b}$$

$$D_{kk} = 2 \left(\frac{1}{k_c} - 2k_c \right) \tanh (k_c h) + \frac{-2h \left(1 + 3k_c^3 \right) + 2h^2 \left(k_c + k_c^3 \right) \tanh (k_c h)}{\cosh^2 (k_c h)} , \tag{A.15}$$

$$
\begin{aligned}
N = {} & \left(\rho_2 U_{2_c}^2 - \rho_1 U_{1_c}^2 \right) \left(3 - \tanh^2 (k_c h)^2 \right) \frac{\Gamma k_c^3}{\tanh (k_c h)} \\
& + \left(\rho_2 U_{2_c}^2 + \rho_1 U_{1_c}^2 \right) \left(1 - 2 \tanh^2 (k_c h) \right) \frac{2k_c^4}{\tanh^2 (k_c h)} \\
& - \left(\rho_2 U_{2_c}^2 + \rho_1 U_{1_c}^2 \right) \frac{h^2 k_c^2}{\sinh^2 (k_c h)} + \frac{3}{2} k_c^5 \tanh (k_c h) ,
\end{aligned} \tag{A.16}
$$

$$F = \frac{\rho_1 U_{1_c}^2 F_0}{\sinh (k_c h)} , \tag{A.17}$$

$$R = k_c^3 \tanh (k_c h) \left(\rho_2 U_{2_c}^2 - \rho_1 U_{1_c}^2 \right) . \tag{A.18}$$

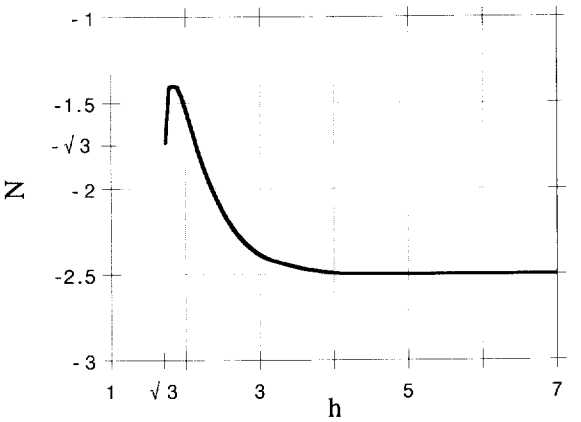

Fig. A.1. Variation of coefficient N of the cubic nonlinear term versus h in the Boussinesq approximation (Eq. (A.21)).

Finally the continuity of particle displacement conditions (A.10a,b) and the boundary conditions (A.11), (A.12) for the mean fields at order ε^3 lead to the following set of evolution equations:

$$\left(\frac{\partial}{\partial T}+U_{2_c}\frac{\partial}{\partial X}\right)\mathcal{H}^{(2)}-h\frac{\partial^2\mathcal{M}_2^{(1)}}{\partial X^2}=0\,, \tag{A.19a}$$

$$\left(\frac{\partial}{\partial T}+U_{1_c}\frac{\partial}{\partial X}\right)\mathcal{H}^{(2)}+h\frac{\partial^2\mathcal{M}_1^{(1)}}{\partial X^2}=0 \tag{A.19b}$$

It is preferable to write the final results in terms of streamwise mean velocity fields $\mathcal{U}_i(X,T)\equiv\partial\mathcal{M}_i^{(1)}/\partial X$. In order to do so, Eq. (A.8) can simply be expressed in terms of $\mathcal{U}_i(X,T)$ by differentiating it once with respect to X, while trivial substitutions can be made to rewrite Eqs. (A.13), (A.19a,b). With a change to the simplified notation $\mathcal{H}^{(2)}\to\mathcal{H}$, $A^{(1)}\to A$, the evolution equations (A.19a,b), (A.8), (A.13) can be cast into the final form:

$$\left(\frac{\partial}{\partial T}+U_{2_c}\frac{\partial}{\partial X}\right)\mathcal{H}-h\frac{\partial\mathcal{U}_2}{\partial X}=0\,,$$

$$\left(\frac{\partial}{\partial T}+U_{1_c}\frac{\partial}{\partial X}\right)\mathcal{H}+h\frac{\partial\mathcal{U}_1}{\partial X}=0\,,$$

$$\frac{\partial\mathcal{H}}{\partial X}-\left(\frac{\partial}{\partial T}+U_{2_c}\frac{\partial}{\partial X}\right)\rho_2\mathcal{U}_2+\left(\frac{\partial}{\partial T}+U_{1_c}\frac{\partial}{\partial X}\right)\rho_1\mathcal{U}_1=S\frac{\partial|A|^2}{\partial X}\,,$$

$$-\tfrac{1}{2}D_{\sigma\sigma}\frac{\partial^2A}{\partial T^2}+\tfrac{1}{2}D_{kk}\frac{\partial^2A}{\partial X^2}=\Delta D_{\Delta U}A+N|A|^2A+Fe^{iqX}+2k_c^2\left(\rho_1U_{1_c}\mathcal{U}_1+\rho_2U_{2_c}\mathcal{U}_2\right)A-R\mathcal{H}A\,.$$

The coefficients $D_{\sigma\sigma}$, $D_{\Delta U}$ and D_{kk} of the linear terms are given by relations (A.14a,b), (A.15). The coefficients N, F, R and S of the various nonlinear terms are given by relations (A.16), (A.17), (A.18) and (A.9) respectively.

If one makes the *Boussinesq approximation* and sets $\rho_1=\rho_2=1/2$, the nonlinear coupling coefficients R and S vanish and one finds for the amplitude equation a forced Klein–Gordon equation as discussed in Section 2. Under this assumption the two remaining nonlinear terms can be written

$$F=\frac{\Delta U_c^2F_0}{4\sinh(k_ch)}\,, \tag{A.20}$$

$$N=\tfrac{3}{2}k_c^5\tanh(k_ch)+\frac{k_c^2\Delta U_c^2}{4}\left(\frac{2k_c^2}{\tanh^2(k_ch)}-4k_c^2+\frac{h^2}{\sinh^2(k_ch)}\right)\,. \tag{A.21}$$

The critical conditions k_c, ΔU_c may be determined from (A.5). By substitution into (A.21), one readily verifies that the coefficient N of the cubic nonlinear term $|A|^2A$ remains negative as long as $h > \sqrt{3}$. The variations of N with the scaled height h are represented on Fig. A.1.

References

[1] Y. Pomeau and P. Manneville, J. Phys. Lett. 40 (1979) 609.
[2] Y. Kuramoto, Chemical Oscillations, Waves and Turbulence (Springer, Berlin, 1984).
[3] P. Manneville, Dissipative Structures, Chaos and Turbulence (Academic Press, Boston, 1990).
[4] A.C. Newell, T. Passot and J. Lega, Ann. Rev. Fluid Mech. 25 (1993) 399.
[5] W. Eckhaus, Studies in Non Linear Stability Theory (Springer, Berlin, 1965).
[6] R.M. Clever and F.H. Busse, J. Fluid Mech. 65 (1974) 625.
[7] A. Pocheau, V. Croquette, P. Legal and C. Poitour, Europhys. Lett. 3 (1987) 915.
[8] H. Riecke and H.G. Paap, Phys. Rev. A 33 (1986) 547.
[9] M.A. Dominguez-Lerma, D.S. Cannell and G. Ahlers, Phys. Rev. A 34 (1986) 4956.
[10] T.B. Benjamin and J.E. Feir, J. Fluid Mech. 27 (1967) 417.
[11] H.C. Yuen and B.M. Lake, Ann. Rev. Fluid Mech. 12 (1980) 303.
[12] E. Fermi, J. Pasta and S. Ulam, Collected papers of Enrico Fermi, Vol. 2, ed. E. Segre (University of Chicago, Chicago, 1965) 978.
[13] J.T. Stuart and R.C. Di Prima, Proc. R. Soc. London, Ser. A 362 (1978) 27.
[14] P. Coullet and S. Fauve, Phys. Rev. Lett. 47 (1985) 2857.
[15] M. Lowe, J.P. Gollub and T.C. Lubensky, Phys. Rev. Lett. 51 (1983) 786.
[16] M. Lowe and J. P Gollub, Phys. Rev. A 31 (1985) 3895.
[17] P. Bak, Rep. Prog. Phys. 45 (1982) 587.
[18] P. Coullet, Phys. Rev. Lett. 56 (1986) 724.
[19] P. Coullet and P. Huerre, Physica D 23 (1986) 27.
[20] P. Coullet and D. Repaux, Europhys. Lett. 3 (1985) 573.
[21] O. Pouliquen, J.M. Chomaz and P. Huerre, Phys. Rev. Lett. 68 (1992) 2596.
[22] S.A. Thorpe, J. Fluid Mech. 32 (1968) 693.
[23] M.A. Weissman, Phil. Trans. R. Soc. Lond. A 290 (1979) 639.
[24] C.G. Lange and A.C. Newell, SIAM J. Appl. Math 21 (1971) 605.
[25] J. Pedlosky, J. Atmos. Sci. 29 (1972) 53.
[26] B. Dubrulle, J.M. Chomaz, S. Kumar and M. Rieutord, Nonlinear stability of slender accretion disks by bifurcation methods, Geophys. Astr. Fluid Dyn, to appear.
[27] P.K. Newton and J.B. Keller, SIAM J. Appl. Math. 45 (1987) 959.
[28] P.K. Newton and J.B. Keller, Wave Motion 10 (1988) 183.
[29] Lord Kelvin, Phil. Mag. 42 (1871) 368.
[30] P.G. Drazin and W.H. Reid, Hydrodynamic Stability (Cambridge Univ. Press, Cambridge, 1981).
[31] J. M Chomaz, P. Huerre and L.G. Redekopp, Bull. Am. Phys. Soc 31 (1986) 1696.
[32] S. Pavithran, Coupling of gravity waves and convection: a natural codimension three problem, Ph.D. dissertation, Department of Aerospace Engineering, University of Southern California, Los Angeles, USA (1991).
[33] S. Pavithran and L.G. Redekopp, The coupling of gravity waves and convection: amplitude equations and planform selection, J. Fluid Mech. (1993), submitted.
[34] A. Davey and K. Stewartson, Proc. R. Soc. A 388, (1974) 191.
[35] V.D. Djordjevic and L.G. Redekopp, J. Fluid Mech. 79 (1977) 703.
[36] Y. Ma and L.G. Redekopp, Phys. Fluids 22 (1979) 1872.
[37] M. Renardy and Y. Renardy, Phys. Fluids, submitted.
[38] O. Pouliquen, J.M. Chomaz and P. Huerre, Propagative Holmboe waves at the interface between two immiscible fluids, J. Fluid Mech. 266 (1994) 277.
[39] C. Elphik, J. Phys. A 19 (1986) L877.
[40] A.C. Newell and J.A. Whitehead, J. Fluid Mech. 38 (1969) 279.
[41] H.C. Yuen and W.E. Ferguson Jr., Phys. Fluids 21 (1978) 1275.
[42] G.L. Lamb, Elements of Soliton Theory (Wiley, New York, 1980).